AGU PUBLICATIONS

Geophysical Research Letters

RESEARCH LETTER
10.1002/2014GL061763

**Key Points:**
- Immediate and delayed inland earthquake activation after Tohoku-oki megathrust
- Seismicity induced by dynamic stress changes through excitation of geofluids
- Earthquake activation pattern correlates with crustal fluid properties

**Supporting Information:**
- Readme
- Figure S1
- Figure S2
- Figure S3
- Figure S4
- Figure S5
- Figure S6
- Text S1

**Correspondence to:**
B. Enescu,
benescu@geol.tsukuba.ac.jp

**Citation:**
Shimojo, K., B. Enescu, Y. Yagi, and T. Takeda (2014), Fluid-driven seismicity activation in northern Nagano region after the 2011 *M*9.0 Tohoku-oki earthquake, *Geophys. Res. Lett.*, *41*, 7524–7531, doi:10.1002/2014GL061763.

Received 4 SEP 2014
Accepted 15 OCT 2014
Accepted article online 20 OCT 2014
Published online 12 NOV 2014

# Fluid-driven seismicity activation in northern Nagano region after the 2011 *M*9.0 Tohoku-oki earthquake

**Kengo Shimojo[1], Bogdan Enescu[2], Yuji Yagi[2], and Tetsuya Takeda[3]**

[1]Graduate School of Life and Environmental Sciences, University of Tsukuba, Tsukuba, Japan, [2]Faculty of Life and Environmental Sciences, University of Tsukuba, Tsukuba, Japan, [3]National Research Institute for Earth Science and Disaster Prevention, Tsukuba, Japan

**Abstract** The dynamic triggering of earthquakes is well documented; however, the underlying physical mechanisms remain obscure. Here we analyze the seismicity in northern Nagano, central Japan, following the Tohoku-oki quake, until the occurrence 13 h later of an $M_w$6.2 local earthquake. We use waveform detection techniques to identify 17 times more earthquakes than those in the Japan Meteorological Agency catalog. The activation of seismicity in the epicentral region of the $M_w$6.2 event is weak and delayed, culminating with the occurrence of the moderate shock preceded by two small foreshocks. The seismicity activation to the south is shallower, abundant, and starts during the passage of Tohoku-oki surface waves of high dynamic stresses. The early activation occurs in areas of relatively high near-surface fluid temperature, indicating that the dynamic triggering is likely caused by excitation of geothermal crustal fluids. The $M_w$6.2 Northern Nagano earthquake might have been delay-triggered by fluid migration from a deep source.

## 1. Introduction

The seismicity in many areas of central and northeastern Japan was activated following the $M_w$9.0 2011 Tohoku-oki earthquake [e.g., *Hirose et al.*, 2011]. While most seismicity changes are consistent with the static stress triggering hypothesis [e.g., *Ishibe et al.*, 2011; *Toda et al.*, 2011; *Enescu et al.*, 2012], either dynamic [*Yukutake et al.*, 2011; *Miyazawa*, 2011] or fluid-related triggering [*Terakawa et al.*, 2013] was invoked to explain the characteristics of earthquake activation in some areas. However, one of the major problems in assessing the role of various triggering factors is the relatively large earthquake catalog incompleteness in the hours following the megathrust event [*Lengliné et al.*, 2012; *Kato et al.*, 2013]. The direct investigation of high-pass filtered waveforms [*Peng et al.*, 2006; *Enescu et al.*, 2007] to detect missing events in the aftermath of a large earthquake is essential for an unbiased interpretation of seismicity.

In this study we focus on the northern Nagano region, central Japan, where an $M_w$6.2 earthquake occurred about 13 h after the Tohoku-oki event. The study area is located about 400 km east of the Tohoku-oki epicentral region. By applying a Matched Filter Technique (MFT) [*Peng and Zhao*, 2009] to the waveform data recorded at the permanent stations in the region, we are able to obtain a much more complete event history, compared with the one catalogued by the Japan Meteorological Agency (JMA). Using this improved catalog, we reveal distinct spatial seismicity activation patterns, which were otherwise impossible to decipher. We also scrutinize continuous high-frequency seismograms recorded by a dense temporary regional network, to detect small events in the very early part of the sequence. Our results bring detailed evidence on the essential role of geothermal activity, as revealed by shallow-depth fluid temperature data, as well as crustal fluid excitation to modulate seismicity activation.

## 2. Data and Method

We use continuous three-component seismic velocity recordings from 10 borehole stations (Figure 1) of the Japanese High Sensitivity Seismograph Network (Hi-net), operated by the National Research Institute for Earth Science and Disaster Prevention (NIED), in the northern Nagano region. All stations are recording at a sampling rate of 100 Hz. Continuous waveforms are 13 h and 15 min long and start on 11 March 2011 at 14:46:00 local time (18 s before the Tohoku-oki main shock origin time) and end on 12 March 2011 at 4:01 local time (about 2 min after the $M_w$6.2 Northern Nagano earthquake). We applied a two-way 10–30 Hz Butterworth filter to the data to reduce the influence of the low-frequency coda wave of the Tohoku-oki main shock, as well as that of aftershocks that occurred at remote distances from northern Nagano.

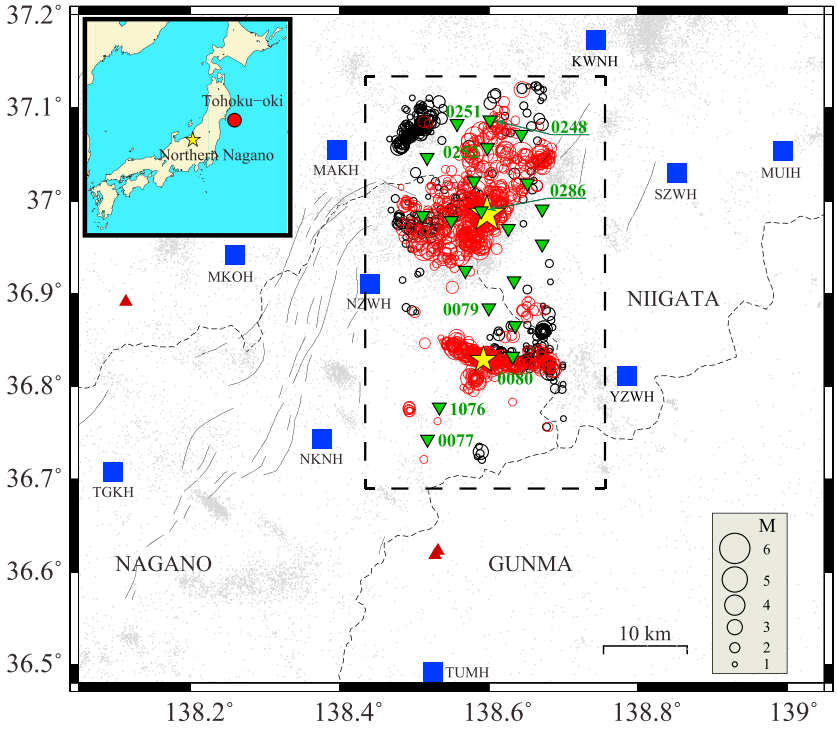


**Figure 1.** Earthquake and station distributions in northern Nagano. The time span of earthquake data is January 2001 to February 2013. The red and black circles indicate the relocated template events ($M \geq 1.0$) that occurred before and after the 2011 Tohoku-oki earthquake, respectively; the gray circles show all the JMA events in a broader region. The blue squares and inverted green triangles represent the Hi-net borehole and temporary surface stations, respectively. The yellow stars show the northern Nagano earthquake and the 12 April 2011 $M_w$5.4 event to the south. The brown triangles show volcanoes. The dotted rectangle delimits our study area. The inset shows the Japanese Islands and the epicenters of the 2011 Tohoku-oki and Northern Nagano earthquakes by red circle and yellow star, respectively. The light dashed lines and thin solid lines show the prefecture borders and faults, respectively.

We use all 1278, $M \geq 1.0$, events of the Hi-net catalogue that occurred between January 2001 and February 2013 in the study region (36.70–37.12°N, 138.44–138.74°E; Figure 1) as template events. To improve the accuracy of the routine earthquake locations, the template earthquakes were relocated using a double-difference approach [*Zhang and Thurber*, 2003] and a regional 3-D velocity model [*Sekiguchi et al.*, 2013]. The earthquakes become shallower by a few kilometers after relocation and more clustered in space. The RMS of the double-difference time residual was reduced from 257 ms to 52 ms. Most events in the hypocentral region of the Northern Nagano earthquake are deeper than 5 km, while those clustered about 10 km to the south (Figure 1) locate in majority from 2 to 5 km depth. We used 4 s long waveform windows for each template event, recorded at each station component, starting 2 s before the *S* wave arrival time, and applied the same filtering as for the continuous data. Only waveforms for which the signal-to-noise (measured as the average waveform amplitude from −6 to −2 s before the *P* wave arrival) ratio is larger than 5 were used for further processing.

We look for events in the continuous data that strongly resemble the template events (Figure S1 in the supporting information). The correlation coefficient between the continuous waveforms and templates, at each recording station (and for each of the three components), is calculated by shifting the template window in increments of 0.01 s. The correlation coefficient value obtained at each time point is assigned to its origin time by subtracting the *S* wave arrival time. Next, we stack the correlation coefficient values for all stations and three components and compute the mean correlation coefficient value at each time point. We then compute the Median Absolute Deviation (MAD) of the mean correlation coefficient trace for each template event and use 9 times the MAD value as the detection threshold [*Peng and Zhao*, 2009]. The location of each waveform-detected event was assigned to be the same as that of the corresponding template earthquake. We end up with a catalogue of 139 events, compared with only 8 in the JMA catalogue, for the 13 h time frame following the Tohoku-oki main shock.

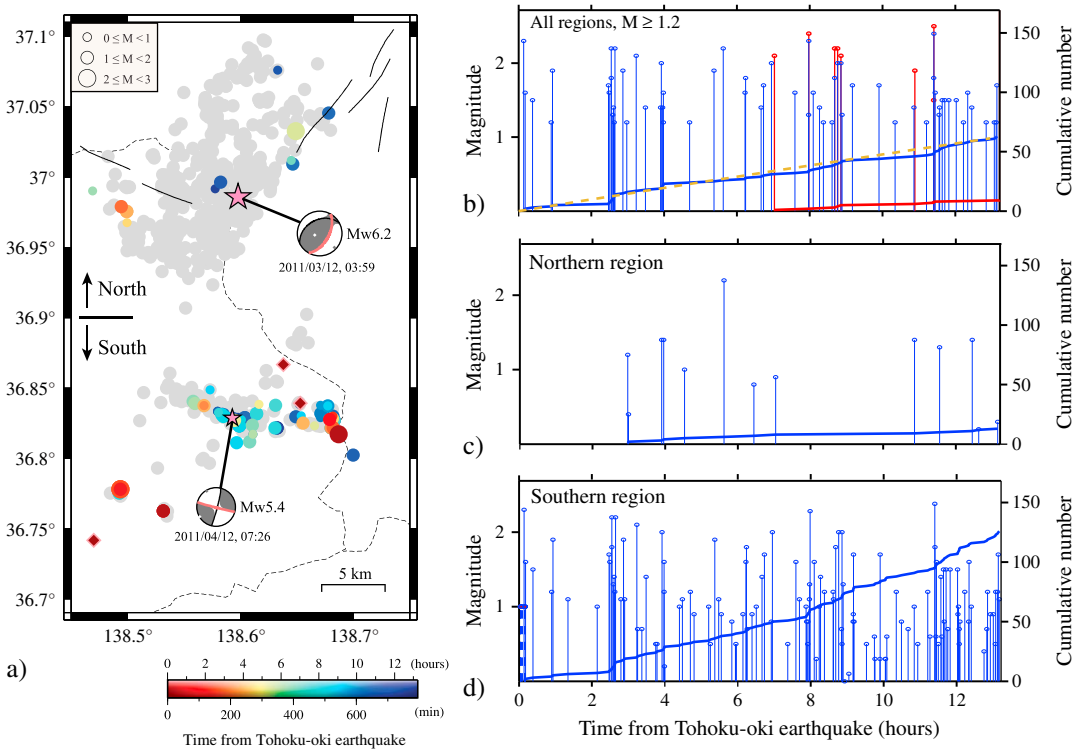


**Figure 2.** Seismicity distribution in the study region: (a) Map view showing the MFT-detected earthquakes, colored as a function of time from the Tohoku-oki megathrust event; the 1 month relocated Hi-net aftershocks are shown in gray. The diamonds represent the early events detected by inspecting the temporary seismic stations in the region. The focal mechanisms of the 12 March 2011 Northern Nagano earthquake and 12 April 2011 event are also shown. The nodal planes on which static stress changes are calculated are colored in red. The "North" and "South" indicate the two regions referred in the text. (b–d) Time history of seismicity for the whole region in Figure 2a and for the "North" and "South" areas, respectively. The stems shown in red in Figure 2b are JMA-catalogued earthquakes, while the dotted line in Figure 2b represents an Omori–Utsu law fit to the data, as explained in the text. The dotted stems in Figure 2c (with red small circle on top) show the events with locations determined by picking *P* and *S* wave arrivals on the temporary and Hi-net seismograms. The solid red and blue lines show the cumulative number of events for detections and JMA catalogue, respectively.

The magnitude of each MFT-detected event was estimated by comparing the waveform amplitudes of detections and templates, assuming that a tenfold increase in amplitude corresponds to one unit increase in magnitude. To minimize the underestimation of larger event magnitudes at high frequencies [e.g., *Shearer*, 2009, Figure 9.24], we use 5 Hz high-pass filtered waveforms for magnitude calibrations.

Since the start of earthquake activation is of primary interest for understanding the triggering mechanism, we have scrutinized continuous waveforms recorded by a dense, regional seismograph network (Figure 1) in the first ~30 min after Tohoku-oki earthquake. Although these stations are installed at the surface and their recordings are relatively noisy, their proximity to the events that occurred in our study area helps the detection of smaller earthquakes. Based on the identified *P* and *S* wave arrivals at both the regional network and Hi-net stations, we have located 7 events that occurred from 130 s to 590 s after the Tohoku-oki earthquake, corresponding roughly with the time period of the main shock surface wave arrivals in northern Nagano.

## 3. Results

Among the 139 MFT detections, only 13 were located in the aftershock area of the $M_w$6.2 earthquake ("North" area), while the majority of the rest were located about 10 km to the south ("South" area) (Figure 2a). Since the station coverage (Figure 1) is about the same for both regions, we are confident that the relatively intense activation in the "South" is genuine.

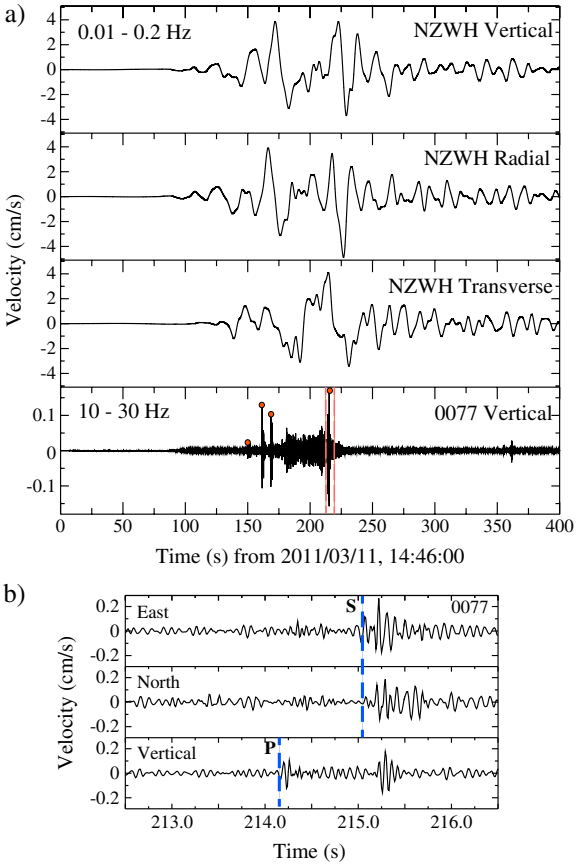


**Figure 3.** Earthquakes detected during the passage of surface waves from the Tohoku-oki earthquake. (a) From top to bottom: low-frequency seismograms (0.01–0.2 Hz) at the NZWH station (vertical, radial, and transverse components) and high-frequency waveform (10–30 Hz) at the temporary station 0077; locally triggered events are marked by small red circles; discontinuous red lines indicate the time interval used for zooming in Figure 3b. (b) Enlarged high-frequency seismogram showing *P* and *S* wave arrivals from one of the triggered events.

The temporal distribution of events (Figures 2b–2d) does not show the characteristic Omori law decay following the occurrence time of Tohoku-oki earthquake. Indeed, a modified Omori law fit (Figure 2b) to the earthquake data in the whole study area, above the completeness magnitude ($M$1.2—Figure S2 in the supporting information), has an unusually low $p$ value (the slope of the modified Omori law distribution) of 0.11, indicating a quasi-constant occurrence rate of events in the Nagano region, during the 13 h observation period (Figure 2b).

In the "North" area, the seismicity is relatively weak, and there are no detections in the first 3 h following the Tohoku-oki earthquake (Figure 2b). A few isolated events occurred 3 to 7 h after the Tohoku-oki main shock but at a distance from the $M_w$6.2 hypocenter. Two small foreshocks occurred close to the hypocenter of the $M_w$6.2 event, within 1 h of its origin time.

In the "South," the seismicity activation is sudden and relatively strong. Note that we have applied the MFT method using the continuous Hi-net waveforms 4 h prior to the Tohoku-oki main shock and found no evidence of local seismicity. The earthquake activity starts immediately after the megathrust event and shows episodic activation, mainly associated with the occurrence of a few larger events ($M \geq 2.0$) (Figure 2d). There is a relative sparseness of seismicity in the first ~2.5 h after the Tohoku-oki earthquake: we attribute it to the difficulty of detecting events of $M$~1.0 due to the very "noisy" waveforms immediately after the $M$9.0 event. The majority of detected earthquakes align along an E-W direction, likely associated with a fault plane of similar strike. Both the strike and dip angles of the southern cluster are consistent with one of the nodal planes of the $M_w$5.4 earthquake, which occurred about 1 month after the $M_w$6.2 Nagano earthquake (Figure S3 in the supporting information). A few small earthquakes also occurred in the southernmost part of our study area (Figure 2a).

As previously mentioned, we have inspected the seismograms recorded by stations of a regional seismic network (installed temporary in the region before the Tohoku-oki event) at early times after the megathrust. Figure 3 shows an example of early event activation recorded in the southernmost area of our study region; the high-pass filtered seismogram (Figure 3a, bottom) at "0077" station (Figure 1) reveals the occurrence of nearby small earthquakes. The earliest event in this area that we were able to locate occurred 131 s after the origin of the Tohoku-oki earthquake, during the passage of the main shock surface waves. Activation at similar early times was also observed within the main "South" cluster (at station "0080"). The earliest event located here occurred ~292 s after the megathrust event. The events located using arrival times observed at both the temporary network and Hi-net stations are plotted as diamonds in Figure 2a. The magnitudes are around 1.0; however, they have relatively large uncertainties. We did not observe similar early activation in the "North," despite the very good station coverage.

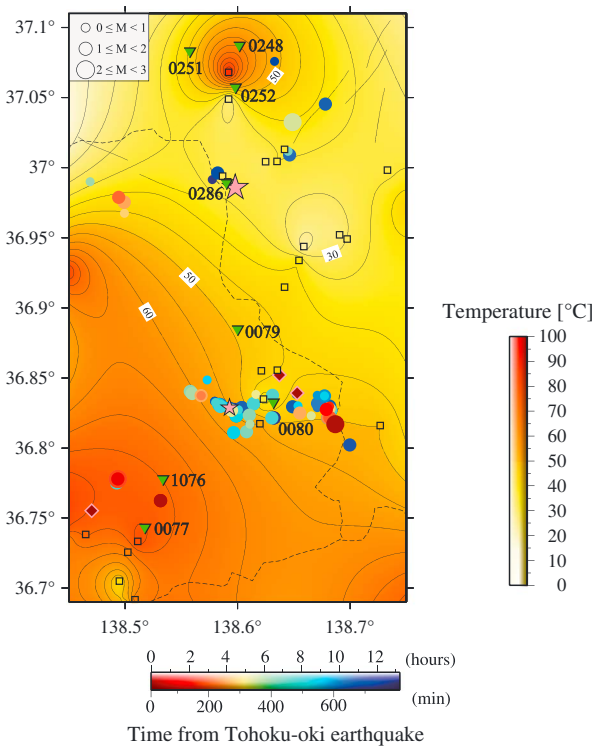


**Figure 4.** Geothermal map of the study area, with seismicity superposed: the temperature distribution (shown by the yellow-to-red color scale in the right side of the map) was obtained by smoothly interpolating locally measured values from locations of small rectangles available all over Japan. The superposed seismicity is the same as in Figure 2. The inverted green triangles show the selected temporary seismic stations. The light dashed lines and thin solid lines show the prefecture borders and faults, respectively.

## 4. Discussion

Several events occurred in the southernmost part of our study region (Figure 2a) during the passage of surface waves (Figure 3a) from the Tohoku-oki earthquake. We estimate the peak dynamic stress changes associated with the passage of Love and Rayleigh waves in the area from the amplitudes of the surface wave ground velocities [e.g., *Peng et al.*, 2009] recorded by the NZWH station (Figure 1). Assuming plane wave propagation for teleseismic waves, the peak dynamic stress $\sigma_d$ is proportional to $Gu'/v_{ph}$ [*Jaeger and Cook*, 1979], where $G$ is the shear modulus, $u'$ is the peak particle velocity, and $v_{ph}$ is the phase velocity. Using a nominal $G$ value of 30 GPa, $v_{ph} = 4.1$ km/s for the Love waves, and $v_{ph} = 3.5$ km/s for the Rayleigh waves, we estimated maximum dynamic stress change values of 300 kPa and 417 kPa, for the Love and Rayleigh waves, respectively. As we discuss in Text S1 of the supporting information, these values might be underestimated; nonetheless, they provide a reliable lower limit for the peak dynamic stress changes in the area. The occurrence of the southernmost earthquakes during the passage of Tohoku-oki surface waves, as well as the significant dynamic stress level, indicates that they were triggered dynamically.

Two main classes of models [*Hill and Prejean*, 2007] are used to explain the triggering by dynamic stresses: (1) direct triggering by frictional failure and (2) triggering through excitation of crustal fluids. As documented in the previous studies, fluids are active agents in geothermal and volcanic areas, which appear to be particularly susceptible to dynamic triggering [*Hill and Prejean*, 2007]. To quantify the degree of geothermal activity in our study region, we use fluid temperature (Figure 4) and flux data [*Geological Survey of Japan*, 2009] measured at the shallowest part of the crust (depth between 0 and 900 m).

As seen in Figure 4, the activated area close to stations "0077" and "1076" is characterized by high fluid temperatures, indicating the presence of a geothermal field. We therefore interpret the dynamically triggered shallow events located close to station "0077" as being caused by a sudden excitation of fluids due to the strong shaking by the Tohoku-oki surface waves. In addition to the temperature data, we have extracted from the same database the fluid flux values of our study region, measured as water flowing through the wells to the surface. The largest such values (~3000 L/min) are observed at the well closest to station "0077," where the most remarkable immediate seismicity activation has occurred (Figure 3 and Figure S4 in the supporting information).

The seismicity activation around station "0080" also started very early after the Tohoku-oki earthquake, although it is only detectable after the passage of the largest-amplitude surface waves. This slight onset delay and the likely weaker early earthquake activation (Figure S4 in the supporting information) may be due to the fact that the area in and around the main "South" cluster is only mildly geothermal (Figure 4). However, the relatively shallow fault-like structure that is revealed by the alignment of seismicity (Figure 2a and Figure S3 in the supporting information) may constitute a favorable permeable environment for geofluid circulation and episodic seismic activity. The results of *Kumazawa and Ogata* [2013], who analyzed the JMA earthquake catalog after the Tohoku-oki main shock, support the swarm-like behavior of seismicity in the "South."

Although the geothermal data used in this study are measured at or close to the surface, there is evidence supporting its relation to thermal properties of the deeper crust. Volcanoes Naeba and Torikabuto, in the southern study region, were active during Quaternary period; such geologically recent volcanic structures are usually warm enough to provide the necessary heat supply for the hot spring activity [e.g., *Fukutomi*, 1961]. We have also checked the geothermal gradient data in Japan, as measured in deep boreholes [*Tanaka*, 2004, and references therein]; however, the measurements were too sparse for mapping purposes. Nevertheless, one observation point located within the southern cluster shows a large geothermal gradient value (~150 K/km), which supports a deeper origin of geothermal activities.

The dynamically initiated triggering of seismicity in the "South" due to crustal fluid excitation is supported also by independent findings [*Terakawa et al.*, 2013] based on the analysis of focal mechanism data in several regions in northeast Japan, which suggest the fault-confined fluid pressure increase in this area, following the Tohoku-oki earthquake. Specifically, *Terakawa et al.* [2013] report a median overpressure coefficient increase of more than 6 times in the "South" Nagano region, following the Tohoku-oki earthquake, which is the largest of all the areas they investigated.

As we have already pointed out, there is no evidence of early seismicity activation in the "North" region; both the MFT analysis and direct examination of waveform data (Figure S4 in the supporting information) support this result. One may question whether the seismicity in the "North" is causally related with the Tohoku-oki earthquake. The strongest argument in favor of a triggering relationship is given by the pre-Tohoku seismicity in the "North": there are no earthquakes of $M \geq 5.5$ from 1 January 1923 (the beginning of the JMA catalogue) to 12 March 2011 Nagano earthquake. It is therefore highly unlikely that the $M_w$6.2 event occurred by chance just 13 h after the Tohoku-oki megathrust. In addition, there have been no recorded earthquakes by JMA in the "North" since 2 March 2011. As shown in Figure 4, the northern area is characterized, in general, by lower fluid temperatures than the "South." One “hotter” area can be seen close to the station “0252.” However, the fluid flux values are relatively low here, and the seismogenic region is relatively deep (between 5 km and 10 km, from the relocated seismicity), so this may explain the lack of dynamically triggered events.

We still need to understand what physical mechanism might have been responsible for the delayed activation of seismicity in the "North," in particular the triggering of the $M_w$6.2 earthquake. *Terakawa et al.* [2013] showed that the region surrounding the Northern Nagano epicenter may have experienced an increase in regional ambient fluid pressure, caused by the flow of overpressurized fluid from a deep reservoir, following the Tohoku-oki earthquake. A tomography study in the area [*Sekiguchi et al.*, 2013] found evidence of a high $v_p/v_s$ structure just below the Northern Nagano hypocentral region, which has been interpreted as a fluid-like body at depth. Such independent results support qualitatively a scenario involving fluid migration from a deeper source, which upon arrival—with some delay—at seismogenic depths could have triggered earthquakes.

Although poorly constrained, the manually located earthquakes in the southernmost part of our study region are shallower than ~5 km. The MFT-detected events in the "South" also have shallower average depths compared to those in the "North" (Figure S5 in the supporting information). The relatively shallow seismogenic areas might be closer to the failure stress threshold, likely due to the geothermal fluid-rich environment; as a consequence, the seismicity activation is pronounced but unlikely to develop into a larger event. The situation is opposite in the hypocentral area of the Northern Nagano earthquake.

Our dynamic stress changes have been estimated using only surface wave amplitudes; however, the orientation of local faults relative to the incidence angle of the incoming surface wave, as well as their faulting mechanism, influences as well the dynamic stresses [*Hill*, 2012]. It is thus possible that the fault structures in the "South" were more favorably oriented for being dynamically triggered than those in the "North."

We have also calculated the static Coulomb failure stress change ($\Delta$CFS) due to slip on the Tohoku-oki earthquake fault plane [*Yagi and Fukahata*, 2011] on two receiver faults: the fault plane of the $M_w$6.2 Northern Nagano earthquake in the "North" and that of the $M_w$5.4 earthquake in the "South," by assuming these two fault planes as representative for the seismicity in the two regions. The obtained $\Delta$CFS values are of 0.02 MPa and 0.13 MPa, respectively (see Text S1 of the supporting information for the details). The value obtained in the "North" is very small (close to the static stress threshold of 0.01 MPa above which earthquake triggering is usually observed [*Parsons et al.*, 2008, and references therein]), and it is doubtful that could have induced an $M_w$6.2 earthquake. For the "South," the static stress changes are significant (~0.13 MPa) but still lower than the peak dynamic stresses (~0.4 MPa).

We cannot exclude the contribution of static stress changes; however, the swarm-like characteristics of seismicity in the "South" suggest that crustal fluids, excited by the dynamic stresses associated with the Tohoku-oki surface waves, are the most important triggering factor.

## 5. Conclusions

We have analyzed the activation pattern of seismicity in the northern Nagano region, central Japan, following the 2011 *M*9.0 Tohoku-oki earthquake. Our investigation period spans about 13 h, between the occurrence times of the megathrust and a local $M_w$6.2 event. The matched filter analysis, applied using event templates and continuous Hi-net waveform data, revealed 17 times more earthquakes than in the JMA catalog. We have also scrutinized continuous waveforms recorded by a local network to identify small and early local events.

The results show distinctive seismicity activation patterns. The epicentral region of the $M_w$6.2 earthquake is characterized by very sporadic activation during the 13 h span, with two small foreshocks within 1 h before the moderate event. The seismicity about 10 km to the south, however, is shallower and shows a significantly stronger and early activation.

The southern locations where seismicity was activated during the passage of surface waves from the megathrust event are nearby a high fluid temperature and fluid flux geothermal hot spot. Other areas of early activation in the south are mildly geothermal. These observations, together with the overall episodic character of seismicity in the southern region, suggest geothermal fluid excitation as the underlying physical mechanism. The seismogenic region of the $M_w$6.2 earthquake, on the other hand, is deeper on average compared with that in the south and located in a region of relatively low near-surface fluid temperatures. We speculate that the $M_w$6.2 Northern Nagano earthquake might have been triggered by fluid migration from a deep source.

**Acknowledgments**

We are grateful to Toshiko Terakawa, Zhigang Peng, Shinji Toda, Kenichiro Hisada, Xiaofeng Meng, and two anonymous reviewers for their useful comments. Toshiaki Tsunogae and Akiko Tanaka helped with the geothermal data, and Zhigang Peng kindly provided his MFT routines. We used the earthquake catalogues provided by JMA and Hi-net, as well as the waveform data of Hi-net and F-Net networks (http://www.hinet.bosai.go.jp/?LANG=en). The MFT-detected earthquake catalogue can be obtained by request from B.E. (benescu@geol.tsukuba.ac.jp). B.E. and Y.Y. acknowledge partial financial support by the "Megathrust Earthquake" project, University of Tsukuba. This study was supported by grant-in-aid for Scientific Research 24540450 and 24310133 of the Japan Ministry of Education, Culture, Sports, Science, and Technology to Y.Y.

The Editor thanks two anonymous reviewers for their assistance in evaluating this paper.

## References

Enescu, B., J. Mori, and M. Miyazawa (2007), Quantifying early aftershock activity of the 2004 mid-Niigata Prefecture earthquake ($M_w$6.6), *J. Geophys. Res.*, *112*, B04310, doi:10.1029/2006JB004629.

Enescu, B., S. Aoi, S. Toda, W. Suzuki, K. Obara, K. Shiomi, and T. Takeda (2012), Stress perturbations and seismic response associated with the 2011 M9.0 Tohoku-oki earthquake in and around the Tokai seismic gap, central Japan, *Geophys. Res. Lett.*, *39*, L00G28, doi:10.1029/2012GL051839.

Fukutomi, T. (1961), On the possibility of volcanic hot springs of meteoric and magmatic origin and their probable life span, *J. Facul. Sci. Hokkaido Univ. Ser. 7 Geophys.*, *1*, 223–266.

Geological Survey of Japan (2009), Geothermal potential map of Japan, CD-ROM version, Digital Geological Map GT-4.

Hill, D. P. (2012), Dynamic stresses, Coulomb failure, and remote triggering – corrected, *Bull. Seismol. Soc. Am.*, *102*, 2313–2336, doi:10.1785/0120120085.

Hill, D. P., and S. Prejean (2007), Dynamic triggering, in *V. 4 Earthquake Seismology*, edited by H. Kanamori, pp. 258–288, Treatise on Geophysics (G. Schubert, Editor in chief), Elsevier, Amsterdam, Netherlands.

Hirose, F., K. Miyaoka, N. Hayashimoto, T. Yamazaki, and M. Nakamura (2011), Outline of the 2011 off the Pacific coast of Tohoku Earthquake (Mw 9.0) — Seismicity: Foreshocks, mainshock, aftershocks, and induced activity —, *Earth Planets Space*, *63*, 513–518.

Ishibe, T., K. Shimazaki, K. Satake, and H. Tsuruoka (2011), Change in seismicity beneath the Tokyo metropolitan area due to the 2011 off the Pacific coast of Tohoku Earthquake, *Earth Planets Space*, *63*, 731–735.

Jaeger, J. C., and N. G. W. Cook (1979), *Fundamentals of Rock Mechanics*, 3rd ed., Chapman and Hall, New York.

Kato, A., J. Fukuda, and K. Obara (2013), Response of seismicity to static and dynamic stress changes induced by the 2011 M9.0 Tohoku-Oki earthquake, *Geophys. Res. Lett.*, *40*, 3572–3578, doi:10.1002/grl.50699.

Kumazawa, T., and Y. Ogata (2013), Quantitative description of induced seismic activity before and after the 2011 Tohoku-Oki earthquake by nonstationary ETAS models, *J. Geophys. Res. Solid Earth*, *118*, 6165–6182, doi:10.1002/2013JB010259.

Lengliné, O., B. Enescu, Z. Peng, and K. Shiomi (2012), Decay and expansion of the early aftershock activity following the 2011, Mw9.0 Tohoku earthquake, *Geophys. Res. Lett.*, *39*, L18309, doi:10.1029/2012GL052797.

Miyazawa, M. (2011), Propagation of an earthquake triggering front from the 2011 Tohoku-Oki earthquake, *Geophys. Res. Lett.*, *38*, L23307, doi:10.1029/2011GL049795.

Parsons, T., C. Ji, and E. Kirby (2008), Stress changes from the 2008 Wenchuan earthquake and increased hazard in the Sichuan basin, *Nature*, *454*, 509–510, doi:10.1038/nature07177.

Peng, Z., and P. Zhao (2009), Migration of early aftershocks following the 2004 Parkfield earthquake, *Nat. Geosci.*, *2*, 877–881, doi:10.1038/ngeo697.

Peng, Z., J. E. Vidale, and H. Houston (2006), Anomalous early aftershock decay rate of the 2004 Mw6.0 Parkfield, California, earthquake, *Geophys. Res. Lett.*, *33*, L17307, doi:10.1029/2006GL026744.

Peng, Z., J. E. Vidale, A. G. Wech, R. M. Nadeau, and K. C. Kreager (2009), Remote triggering of tremor along the San Andreas Fault in Central California, *J. Geophys. Res.*, *114*, B00A06, doi:10.1029/2008JB006049.

Sekiguchi, S., et al. (2013), Onshore earthquake observations, in *The Annual Report of the Multidisciplinary Research Project for Investigations in the High Strain Rate Zone of Japan*, pp. 11–49, Research and Development Bureau of MEXT, Japan, and NIED.

Shearer, P. (2009), *Introduction to Seismology*, 2nd ed., Cambridge Univ. Press, Cambridge, U. K.

Tanaka, A. (2004), Geothermal gradient and heat flow data in and around Japan (II): Crustal thermal structure and its relationship to seismogenic layer, *Earth Planets Space*, *56*, 1195–1199.

Terakawa, T., C. Hashimoto, and M. Matsu'ura (2013), Changes in seismic activity following the 2011 Tohoku-oki earthquake: Effects of pore fluid pressure, *Earth Planet. Sci. Lett.*, *365*, 17–24, doi:10.1016/j.epsl.2013.01.017.

Toda, S., R. S. Stein, and J. Lin (2011), Widespread seismicity excitation throughout central Japan following the 2011 M=9.0 Tohoku earthquake and its interpretation by Coulomb stress transfer, *Geophys. Res. Lett.*, *38*, L00G03, doi:10.1029/2011GL047834.

Yagi, Y., and Y. Fukahata (2011), Rupture process of the 2011 Tohoku-oki earthquake and absolute elastic strain release, *Geophys. Res. Lett.*, *38*, L19307, doi:10.1029/2011GL048701.

Yukutake, Y., R. Honda, M. Harada, T. Aketagawa, H. Ito, and A. Yoshida (2011), Remotely-triggered seismicity in the Hakone volcano following the 2011 off the Pacific coast of Tohoku Earthquake, *Earth Planets Space*, *63*, 737–740.

Zhang, H., and C. H. Thurber (2003), Double-Difference tomography: The method and its application to the Hayward fault, California, *Bull. Seismol. Soc. Am.*, *93*, 1875–1889.